Neural activity and CaMKII protect mitochondria from fragmentation in aging *Caenorhabditis elegans* neurons

Hao-Ching Jiang[a,1], Jiun-Min Hsu[a,1], Chien-Ping Yen[a], Chi-Chao Chao[b], Ruey-Hwa Chen[a,c], and Chun-Liang Pan[a,2]

[a]Institute of Molecular Medicine, National Taiwan University, 10002 Taipei, Taiwan; [b]Department of Neurology, National Taiwan University Hospital, 10002 Taipei, Taiwan; and [c]Institute of Biological Chemistry, Academia Sinica, 11529 Taipei, Taiwan

Edited by Martin Chalfie, Columbia University, New York, NY, and approved June 8, 2015 (received for review January 28, 2015)

Decline in mitochondrial morphology and function is a hallmark of neuronal aging. Here we report that progressive mitochondrial fragmentation is a common manifestation of aging *Caenorhabditis elegans* neurons and body wall muscles. We show that sensory-evoked activity was essential for maintaining neuronal mitochondrial morphology, and this activity-dependent mechanism required the Degenerin/ENaC sodium channel MEC-4, the L-type voltage-gated calcium channel EGL-19, and the Ca/calmodulin-dependent kinase II (CaMKII) UNC-43. Importantly, UNC-43 phosphorylated and inhibited the dynamin-related protein (DRP)-1, which was responsible for excessive mitochondrial fragmentation in neurons that lacked sensory-evoked activity. Moreover, enhanced activity in the aged neurons ameliorated mitochondrial fragmentation. These findings provide a detailed description of mitochondrial behavior in aging neurons and identify activity-dependent DRP-1 phosphorylation by CaMKII as a key mechanism in neuronal mitochondrial maintenance.

mitochondria | neuronal aging | neural activity | *C. elegans* | CaMKII

The role of mitochondria in cellular senescence is complex in that they could be the target of aging process, or they directly contribute to the progression of cellular aging (1). Mitochondria undergo dynamic transition between more connected network-like patterns and smaller, isolated forms (2). In yeast and fungi, mitochondrial fragmentation emerged early during aging (3, 4). By contrast, swollen or "giant" mitochondria had been documented in aging mouse hepatocytes or *Caenorhabditis elegans* muscles (5, 6). These studies suggest that altered mitochondrial morphology is a core component of eukaryotic cellular aging, but they also highlight the heterogeneity of age-dependent mitochondrial morphological defects.

Excessive mitochondrial fragmentation may result from an imbalance between fusion and fission, which are mediated primarily by two classes of GTPases structurally related to dynamins: Mitofusins (MFNs)/Fzo1/FZO-1 and Drp1/DRP-1, respectively (2). Mitofusins and Drp1 are both targets of regulation by a wide range of physiological and stress signals, such as genotoxic stress-induced MFN2 degradation or inflammation-dependent Drp1 activation (7). The identity of physiological signals that maintain mitochondrial morphology during neuronal aging is largely unknown.

Electrical activity is crucial for several developmental events in the nervous system, including axon pathfinding, synaptic remodeling, and specification of the neurochemical phenotype of neurons (8). Altered membrane excitability and intracellular calcium dynamics could be found in mammalian neurons at old age (9, 10). In *C. elegans* neurons, evoked activity is essential to prevent premature deterioration of neuronal structures during aging (11). It had been shown that mitochondria in the cultured mammalian neurons underwent fragmentation upon forced membrane depolarization or inhibition of protein kinase A (PKA) (12, 13). Because PKA could also be regulated through neuronal activation, these observations raise the possibility that neural activity maintains neuronal structures during aging at least in part by regulating mitochondrial morphology and functions. In the current study, we directly address this possibility and demonstrate that sensory-evoked activity is essential to counteract age-dependent mitochondrial fragmentation in *C. elegans* neurons, likely by inhibiting the mitochondrial fission protein DRP-1.

Results

Mitochondria Were Progressively Fragmented in Aging *C. elegans* Neurons. We visualized mitochondria in *C. elegans* by expressing TOMM20::mCherry ("mito::mCherry"), which targets mitochondrial outer membrane, in the touch mechanosensory neurons (Fig. 1 *A* and *B*) or the thermosensory neuron AFD (Fig. S1 *A* and *B*). In the neurons of L4 and young adult animals, mitochondria in the cell body showed networked morphology, which became progressively fragmented with age (Fig. 1 *A* and *B* and S1). Similar changes were documented in the body wall muscles (Fig. S1 *C* and *D*). It is possible that background, nonmitochondrial mCherry produces the illusion of connected mitochondria, or that mitochondria are still connected in those seemingly isolated mito::mCherry puncta, but somehow those connections are below the detection sensitivity. To rule out these possibilities, we assayed fluorescence recovery after photobleaching (FRAP) (Fig. 1 *C* and *D*). Because mito::mCherry was inserted into the mitochondrial outer membrane, FRAP in a region of interest (ROI) of the networked mitochondrion depended on diffusion of unbleached mito::mCherry through membrane continuity. By contrast, FRAP in the ROIs of isolated mitochondria depended on new mito::

Significance

Structural and functional deterioration of neurons underlie the progressive decline in cognitive and behavioral functions associated with aging. In this study, we found that progressive fragmentation of mitochondria is a hallmark of neuronal aging in *Caenorhabditis elegans*. Progression of mitochondrial fragmentation is influenced by lifespan and is specifically regulated by neural activity. Loss of sensory-evoked activity worsened age-dependent mitochondrial fragmentation, whereas increased sensory-evoked activity improved it. We showed that sensory-evoked activity maintained mitochondrial morphology by inhibiting the mitochondrial fission protein, dynamin-related protein 1 through phosphorylation at a conserved amino acid residue. These findings contribute to mechanistic understanding of neuronal aging and identify sensory-evoked activity as a critical regulator of neuronal mitochondria during aging.

Author contributions: H.-C.J., J.-M.H., R.-H.C., and C.-L.P. designed research; H.-C.J., J.-M.H., C.-P.Y., C.-C.C., R.-H.C., and C.-L.P. performed research; H.-C.J., J.-M.H., C.-P.Y., R.-H.C., and C.-L.P. analyzed data; and H.-C.J. and C.-L.P. wrote the paper.

The authors declare no conflict of interest.

This article is a PNAS Direct Submission.

[1]H.-C.J. and J.-M.H. contributed equally to this work.

[2]To whom correspondence should be addressed. Email: chunliangpan@gmail.com.

This article contains supporting information online at www.pnas.org/lookup/suppl/doi:10.1073/pnas.1501831112/-/DCSupplemental.

www.pnas.org/cgi/doi/10.1073/pnas.1501831112

Downloaded at Palestinian Territory, occupied on December 13, 2021

www.manaraa.com

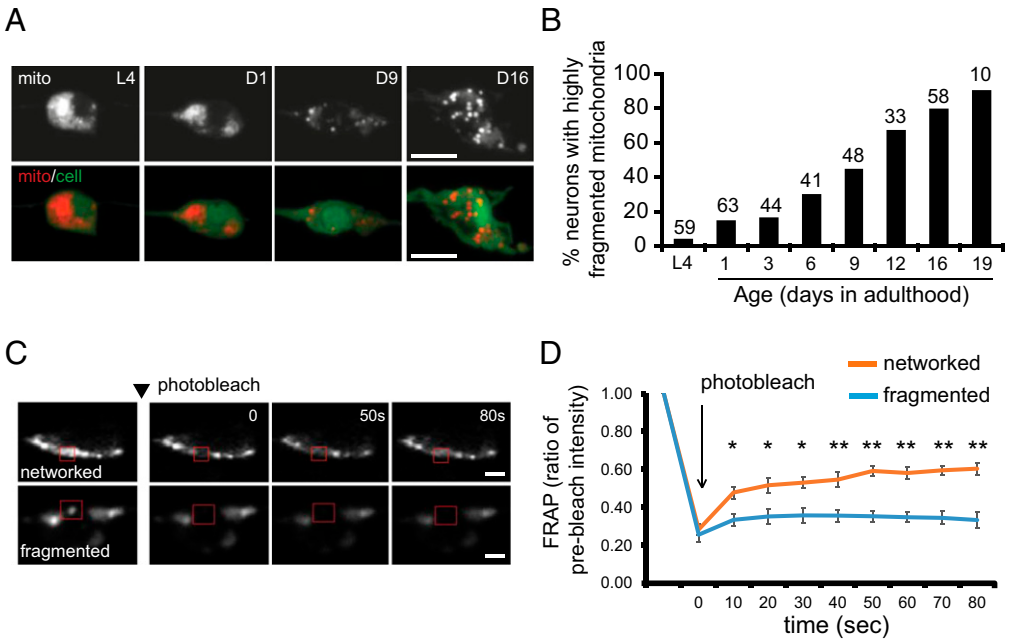

Fig. 1. Age-dependent mitochondrial fragmentation in *C. elegans* touch neurons. (*A*) Projected confocal z-stack images of mitochondria in the ALM touch neurons visualized with mito::mCherry. (*B*) Quantification of neurons with highly fragmented (>50%) mitochondria in the touch neuron soma. *n* = numbers of neurons scored. See *SI Materials and Methods* for detail of data analysis. (*C*) Representative images of FRAP from D4 ALM neurons. Regions subjected to photobleaching were boxed. (*D*) Quantification of FRAP from D4 ALM neurons. *n* = 10 and 12 regions of interest (ROIs) on mitochondria for the networked or fragmented categories, respectively. $*P < 0.05$, $**P < 0.01$, Mann–Whitney *u* test. (Scale bars: *A*, 5 μm; *C*, 1 μm.)

mCherry synthesis and insertion into mitochondrial outer membrane, or on fusion with nearby, unbleached mitochondria. In D4 animals, we observed significantly greater FRAP for ROIs in networked mitochondria than that for ROIs on isolated mitochondria (Fig. 1 *C* and *D*). These findings confirm the use of mito::mCherry as a faithful reporter for the connectivity of mitochondrial outer membrane and suggest that progressive mitochondrial fragmentation is a hallmark of neuronal aging in *C. elegans*.

We previously reported that the processes of touch neurons developed age-dependent defects, including bubble-like lesions or beading (11). It had been shown that neurite beadings in old *C. elegans*-contained mitochondria (14). We confirmed this finding and additionally observed that large bubble-like lesions tended to accumulate mitochondria at the ends, rather than in the center, of the lesion (Fig. S2*A*). By quantitative time-lapse imaging, we found no significant changes in the movement patterns of mitochondria in the old touch neurons (Fig. S2 *B* and *C*). Therefore, for subsequent analysis, we focused on mitochondria in the cell body of the touch neurons.

Fragmented Mitochondria Were More Oxidized and Were Targeted to Lysosomes. To understand whether altered mitochondrial morphology implicates functional deterioration, we measured the oxidation-reduction status of mitochondrial matrix with roGFP, a GFP variant that increases brightness in a more oxidized environment (15). We targeted roGFP to the mitochondrial matrix in the touch neurons (Fig. 2*A*), and found that compared with that in the young neurons, roGFP signals were significantly increased in the old neurons, suggesting more oxidized mitochondrial matrices (Fig. 2 *A* and *B*). Together with the morphological analysis, these results indicate that mitochondria in *C. elegans* neurons deteriorate, both in morphology and function, during aging.

Mitochondrial fragments were often targeted for lysosomal degradation (16). To test whether mitochondrial fragments in aged neurons were recruited to lysosomes, we monitored the colocalization of mitochondria with lysosomes, using the lysosomal reporter LMP-1/LAMP::GFP (Fig. 2*C*). In young neurons where mitochondria were mostly networked, LMP-1::GFP signal occasionally colocalized with mito::mCherry (Fig. 2*C*). By contrast, extensive colocalization between LMP-1::GFP and mito::mCherry signal was observed in aged touch neurons (Fig. 2*C*). No such colocalization was found between mitochondria and the Golgi apparatus in young or old neurons (Fig. S2*D*). These results show that fragmented mitochondria in aged *C. elegans* touch neurons were recruited to lysosomes for degradation.

Longevity Mutations Altered Mitochondrial Morphology in Accordance with Life Span Changes. Neuronal aging in *C. elegans* could be regulated both by signaling pathways that regulate organismal life span and influence tissue aging cell nonautonomously (17). To understand how life span influences mitochondrial during neuronal aging, we studied mitochondrial morphology in mutant strains with altered life span. Mutations in the heat shock transcription factor gene *hsf-1* reduce life span and trigger premature neuronal aging (11, 18, 19). We found that in the *hsf-1* mutant, mitochondrial fragmentation progressed rapidly compared with the wild type (Fig. 3). By contrast, mutations in *daf-2*, which encodes the sole insulin-like growth factor-1 (IGF1) receptor in *C. elegans*, increase life span and slow neuronal aging (11, 14, 20–22). *daf-2* mutations also significantly attenuated mitochondrial fragmentation in the aged touch neurons (Fig. 3). Together these observations indicate that neuronal mitochondrial morphology is under the systemic influence of longevity genes.

Sensory-Evoked Activity Maintains Mitochondrial Morphology Through the L-Type VGCC and CaMKII. We had previously reported that neural activity contributed to neuronal maintenance during aging (11). We found that sensitivity to light touch, a function that requires intact touch neurons, decreased in the aged wild-type animals before obvious locomotion defects were observed (Fig. S3*A*). This observation prompted us to test whether sensory-evoked activity also maintains mitochondria in the touch neurons. Mutations

Downloaded at Palestinian Territory, occupied on December 13, 2021

www.manaraa.com

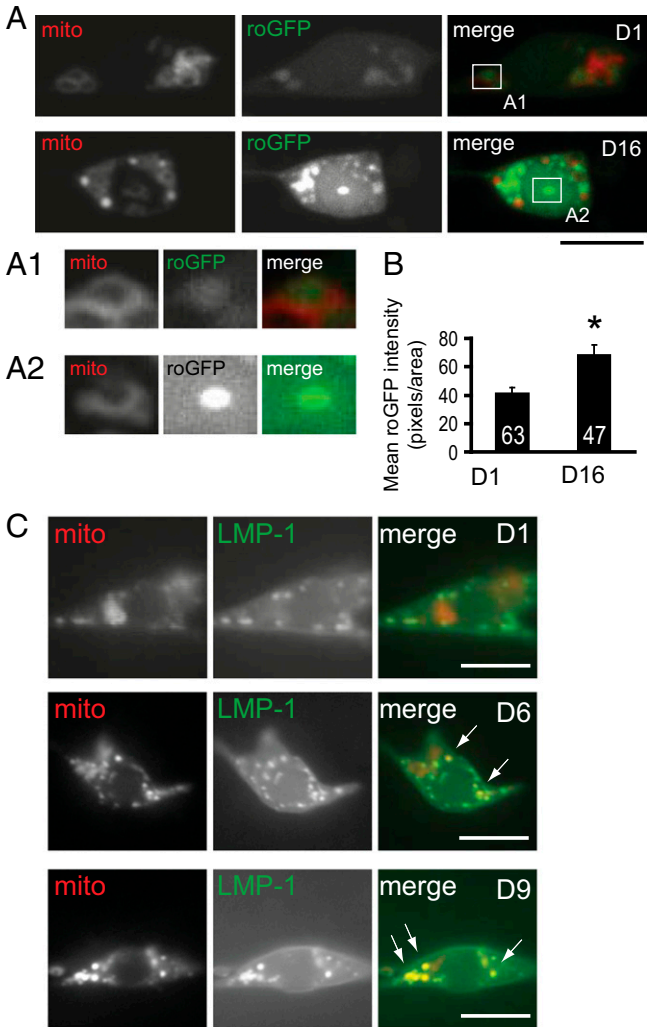

Fig. 2. Mitochondrial oxidation, lysosomal recruitment, and disrupted ER-Mitochondrial contact during neuronal aging. (*A*) Projected z-stack confocal fluorescence images of touch neurons expressing roGFP and mito::mCherry. Select mitochondria (A1 and A2) were highlighted to demonstrate roGFP (matrix) and mito::mCherry (outer mitochondrial membrane). (*B*) Quantification of roGFP intensity. $*P < 0.01$, Student's *t* test. *n* = numbers of mitochondria quantified for roGFP signal intensity. Error bars are SE of means. (*C*) Fluorescence images of touch neurons expressing mito::mCherry and LMP-1::GFP (lysosomes). Arrows are foci of colocalization between mitochondria and lysosomes. (Scale bars: 5 μm.)

in *mec-4*, which encodes a Degenerin/epithelial sodium channel (DEG/ENaC) protein essential for touch neuron activation (23), resulted in accelerated mitochondrial fragmentation in these cells (Fig. 4*A*). Touch neuron-specific expression of the human voltage-gated potassium channel, hKv1.1, rendered the animal touch-insensitive and resulted in premature mitochondrial fragmentation and neuronal aging (Fig. 4*A* and Fig. S3 *B–D*). Expression of hKv1.1 in the touch neurons of the *mec-4* mutant did not further increase mitochondrial fragmentation (Fig. 4*A*), suggesting that sensory-evoked activity is the predominant component of neural activity that maintains mitochondria in the touch neurons. By contrast, *mec-4* expression in the touch neurons rescued mitochondrial fragmentation, touch sensitivity, and neuronal morphology of the *mec-4* mutant (Fig. 4*A* and Fig. S3 *B–D*). Moreover, it also significantly improved touch sensitivity and mitochondrial morphology of the aged wild-type animals (Fig. 4*A* and Fig. S3*A*). These experiments indicate that sensory-evoked activity acts cell-autonomously to maintain mitochondrial morphology in the aging touch neurons.

The *C. elegans* L-type voltage-gated calcium channel (L-VGCC) EGL-19 is required for normal sensory-evoked calcium influx in the touch neuronal soma (24, 25). We found that in the *egl-19* reduction-of-function mutant, mitochondria in the touch neurons were prematurely fragmented in a way similar to that in the *mec-4* mutant (Fig. 4*B*). Moreover, mitochondrial fragmentation in the *egl-19; mec-4* double mutant was comparable to that in either *mec-4* or *egl-19* single mutant, suggesting that MEC-4 and EGL-19 function in a common pathway (Fig. 4*B*).

One of the major targets of evoked calcium influx in the neurons are Ca^{2+}/calcmodulin-dependent kinases (CaMK), and CaMKI had been reported to regulate mitochondrial dynamics in cultured mammalian neurons (13). Of the *C. elegans* CaMKs, both the CaMKI/IV *cmk-1* and the CaMKII *unc-43* were robustly expressed in the nervous system, including the touch neurons (26, 27). We found that mitochondrial fragmentation was increased in the touch neurons of the *unc-43* mutant but not the *cmk-1* mutant (Fig. 4*C* and Fig. S4*A*). Mitochondrial defects were not further worsened in the *unc-43; mec-4* double mutant, compared with those of the *mec-4* or the *unc-43* single mutant (Fig. 4*C*). To confirm that UNC-43 acts downstream of membrane activity in mitochondrial maintenance, we expressed a gain-of-function UNC-43, UNC-43(E108K/GF), whose activity was largely calcium-independent. Expression of UNC-43(GF) in the touch neurons rescued mitochondrial morphology of the *mec-4* mutant (Fig. 4*C*). Moreover, many young neurons that expressed UNC-43(GF) contained mitochondria of elongated tubular morphology (Fig. 4*D*). Together these experiments suggest that sensory-evoked activity maintains mitochondrial morphology in *C. elegans* neurons through L-type VGCC and CaMKII. By contrast, touch insensitivity of the *mec-4* mutant was not improved by UNC-43(GF) (Fig. S3*B*). These results indicate that touch responses and mitochondrial regulation represent two distinct physiological processes controlled by sensory-evoked activity in the touch neurons, and they could be genetically uncoupled.

DRP-1–Mediated Mitochondrial Defects in Activity-Deficient Neurons. Mitochondrial morphology is regulated by genes encoding dynamin-related GTPases, the profission Drp1 and the profusion Mfn2 and Opa1 (2). Their *C. elegans* homologs are *drp-1*, *fzo-1,* and *eat-3*, respectively (28–30). We examined mitochondrial morphology in the *drp-1* null mutant, and found that age-dependent mitochondrial fragmentation in the *drp-1* mutant was similar to that of the wild type (Fig. 5*A* and Fig. S4*B*). This result suggests that age-dependent mitochondrial fragmentation is not caused by inadvertent DRP-1 activity. Mitochondria were almost completely

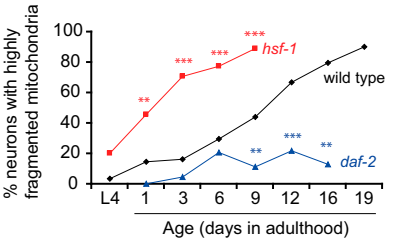

hsf-1 (n)	15	42	27	35	54	NA	NA	NA
wild type (n)	59	63	44	41	48	33	58	10
daf-2 (n)	NA	47	45	29	36	46	31	NA

Fig. 3. Mitochondrial morphology in longevity mutants. Quantification of highly fragmented mitochondria in the touch neurons of the wild type, *hsf-1*, or *daf-2*. Data for the wild type were replotted from those in Fig. 1*B*. *n* = numbers of neurons scored. $**P < 0.005$; $***P < 0.0001$, Fisher's exact test or two-proportion z test. NA, not assessed.

Downloaded at Palestinian Territory, occupied on December 13, 2021
www.manaraa.com

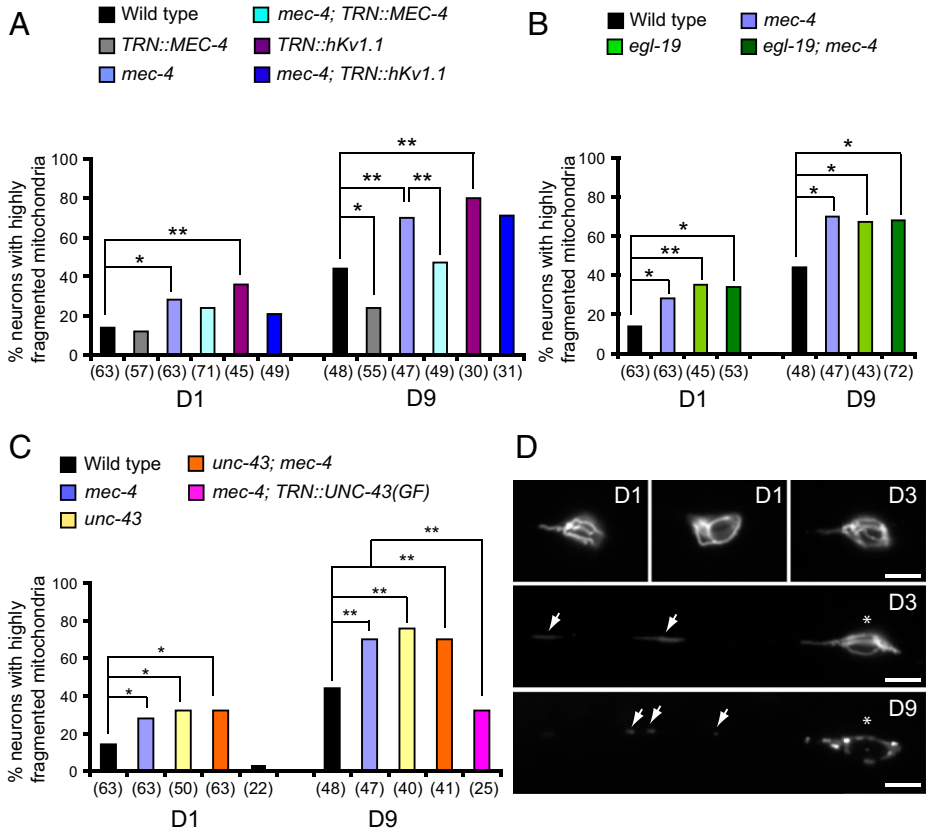

Fig. 4. Neural activity maintains mitochondrial morphology through VGCCs and CaMKII. (*A*–*C*) Quantification of highly fragmented mitochondria in the touch neurons of the wild type as well as *mec-4* (*A*), *egl-19* (*B*), or *unc-43* mutants (*C*). *TRN* is the *mec-7* promoter. *n* = numbers of neurons scored. $*P < 0.05$; $**P < 0.01$, two-proportion z test. (*D*) Elongated mitochondria in the ALM neurons of the *mec-4* mutants overexpressing UNC-43(GF). Epifluorescence images were shown, with arrows and asterisks indicating mitochondria and the ALM soma, respectively. (Scale bars: 5 μm.)

fragmented in the *fzo-1* deletion mutant since day 1 of adulthood (Fig. S4*C*), precluding us from testing genetically the alternative hypothesis that age-dependent loss of FZO-1 function drives progressive mitochondrial fragmentation in aging neurons.

Surprisingly, the *drp-1* mutation significantly reduced excessive mitochondrial fragmentation in the touch neurons of the *mec-4* mutant (Fig. 5*A*), suggesting that increased DRP-1 activity accounts for exaggerated mitochondrial fragmentation in electrically silenced neurons. Of note, the *drp-1* mutation did not improve touch insensitivity of the *mec-4* mutant (Fig. S3*B*). An N terminus-tagged GFP::DRP-1 fusion protein caused excessive mitochondrial fragmentation when expressed in the touch neurons at low level (Fig. 5 *A* and *B*). Discrete GFP::DRP-1 puncta could be found both in the neurite and the cytosol (Fig. 5 *B* and *C*), and some GFP::DRP-1 puncta were associated with the ends of mitochondria in the neurite (Fig. 5*C*).

UNC-43/CaMKII Inactivates DRP-1 by Phosphorylation. We speculate that neural activity inhibits DRP-1 function, likely through CaMKII-dependent DRP-1 phosphorylation. Two potential motifs for CaMK phosphorylation, centering on threonine 613 and serine 590, could be found in DRP-1 (Fig. 5*D*). T613, which is equivalent to serine 637 (S637) of human Drp1, is also a phosphorylation target of protein kinase A, and S637 phosphorylation inhibits mammalian Drp1 activity (12). By contrast, the mammalian serine 616, equivalent to S590 of DRP-1, was phosphorylated by CaMKI in an activity-dependent manner, and this phosphorylation-activated Drp1 (13, 31). To test whether *C. elegans* DRP-1 is a substrate for UNC-43/CaMKII, we performed in vitro kinase assay with purified HA-tagged UNC-43 and GFP::DRP-1 (Fig. 5*E* and Fig. S5). We found that UNC-43 was able to phosphorylate DRP-1 in vitro (Fig. 5*E* and Fig. S5). Phosphorylation was reduced but not abolished with DRP-1(T613A), suggesting that UNC-43 phosphorylates T613 and also additional residues of DRP-1 (Fig. 5*E* and Fig. S5).

Next, we tested whether T613 phosphorylation inhibits DRP-1 biological activity. Expression of the phosphomimetic DRP-1 (T613D) failed to modify the mitochondrial phenotypes of the *drp-1; mec-4* mutant (Fig. 5*A*). By contrast, the phosphorylation-resistant DRP-1(T613A) significantly increased mitochondrial fragmentation in the *drp-1; mec-4* mutant (Fig. 5*A*). We also tested DRP-1(S590D) and DRP-1(S590A) and found that both were functional because they complemented the loss of *drp-1* in the *drp-1; mec-4* double mutant (Fig. 5*A*). This result implies that T613 phosphorylation inhibits DRP-1 activity. Together these data indicate that phosphorylation of *C. elegans* DRP-1 at T613, by the action of UNC-43/CaMKII, reduces its biological activity and protects neuronal mitochondria from excessive fragmentation in *C. elegans*.

Discussion

Our previous work showed that neural activity maintains neuronal structures during *C. elegans* aging (11), but the molecular pathways that interpret membrane activation as a neuroprotective signal for aging are largely unclear. Compromised mitochondrial morphology and function had been implicated in aging, but physiological signals that maintain mitochondrial integrity in this context are incompletely understood. Here, we demonstrated that sensory-evoked activity maintains mitochondrial morphology by inhibiting DRP-1, via CaMKII-dependent DRP-1 phosphorylation

Downloaded at Palestinian Territory, occupied on December 13, 2021
www.manaraa.com

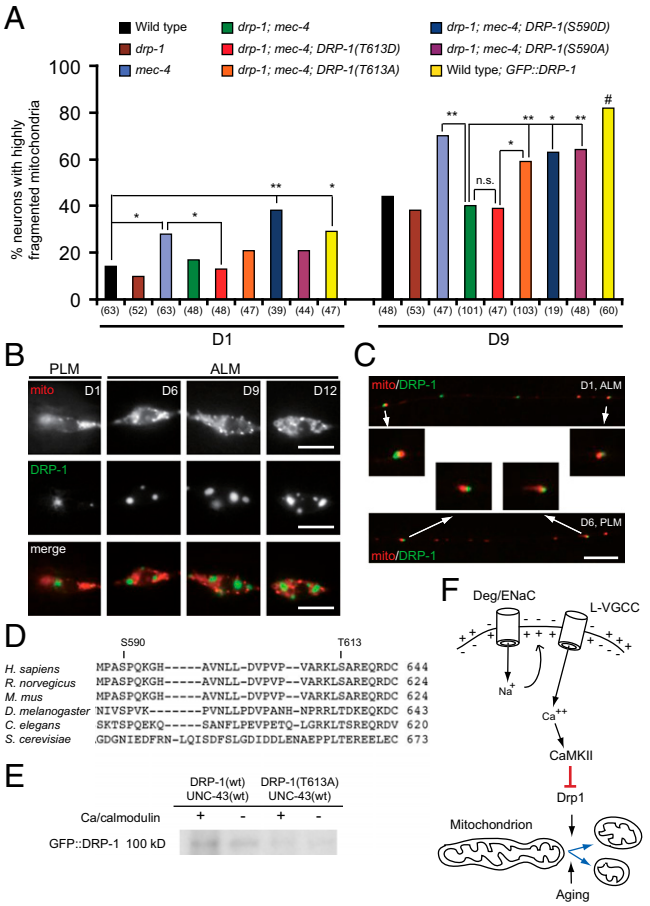

Fig. 5. CaMKII maintains mitochondrial morphology by phosphorylating and inhibiting DRP-1. (*A*) Quantification of highly fragmented mitochondria in the touch neurons. $*P < 0.05$; $*P < 0.01$, two-proportion z test; $\#P < 0.05$, Fisher's exact test, wild type vs. wild type with GFP::DRP-1. *n* = numbers of neurons scored. (*B*) Epifluorescence images of touch neurons expressing mito::mCherry and GFP::DRP-1. (*C*) GFP::DRP-1 in the PLM neurite. Select DRP-1 puncta were enlarged to show the close association of GFP::DRP-1 with mitochondria. (*D*) DRP-1 sequence alignment of various species. For *C. elegans*, DRP-1b is shown. (*E*) In vitro kinase assay of DRP-1 by UNC-43. (*F*) Schematic model of mitochondrial maintenance by activity-dependent Drp1/DRP-1 inhibition. Unknown, age-dependent factors contribute to mitochondrial fragmentation independently of Drp1 in wild-type neurons. (Scale bars: *B*, 5 μm; *C*, 10 μm.)

(Fig. 5*F*). These findings link sensory-evoked activity to the maintenance of mitochondrial morphology. Our data suggest that UNC-43/CaMKII phosphorylates DRP-1 at T613 (S637 of human Drp1) and inhibits DRP-1. While the current study was under review, a study in brain tumor cells revealed a similar role for CaMKII in phosphorylating and inhibiting Drp1 (32). S637 phosphorylation of mammalian Drp1 by PKA inhibits DRP-1 activity and protects neurons from apoptosis induced by mitochondrial respiratory inhibition (12). Taken together, these findings indicate that S637/T613 phosphorylation of Drp1/DRP-1 is likely a conserved neuroprotective mechanism. It is important to note that in an earlier study using mammalian neurons, Han et al. found that forced membrane depolarization triggered mitochondrial fragmentation by S616 phosphorylation of Drp1 (equivalent to S590 in *C. elegans* DRP-1b) via CaMKIα (13). Consistent with this observation, we found that the phosphomimetic DRP-1(S590D) was functional and complemented *drp-1* loss in the *drp-1; mec-4* double mutant. These observations indicate that diverse physiological signals, including neural activity of distinct spatial and temporal patterns, promote or inhibit Drp1 activity by differential phosphorylation at specific residues.

In an earlier study, elimination of the Drp1 homolog in *Neurospora* rescued age-dependent mitochondrial fragmentation and extended longevity (3). However, we found that age-dependent mitochondrial fragmentation in the wild-type neurons was not significantly ameliorated by removing *drp-1* activity, suggesting that factors other than *drp-1* are responsible for deteriorated mitochondrial morphology in the wild type. Although response to light touch decreased with aging, it was far less severe than that in animals lacking the mechanosensory transduction channel MEC-4. This finding indicates that residual neural activity in middle-aged neurons is sufficient to inhibit DRP-1 activity. One interesting candidate that maintains mitochondrial integrity in the wild type is Mitofusin/MFN, which had been implicated in maintaining longevity in *Neurospora* (33). The progressive fragmentation of mitochondria in aging tissues is also consistent with age-dependent loss of MFN level or activity. Important issues in the future are how endogenous MFN level and activity change in the course of neuronal aging, and whether neural activity promotes MFN functions to maintain mitochondrial morphology.

Materials and Methods

Microscopy, Mitochondrial Scoring, and Quantification of Fluorescence Signals. Animals cultured at 20 °C (and 15 °C for *cmk-1*, for *cmk-1* showed life span deficits at 20 °C) were anesthetized with 1 mM levamisole and mounted on 5% (wt/vol) agarose pad. For mitochondrial scoring, epifluorescence or confocal images were acquired by using the 63x Carl Zeiss Apochromat objective (Zeiss AxioImager M2 or LSM700 Confocal System). Mitochondrial morphology in the neuronal soma was classified as: grade 0, no fragmentation; grade 1, < 50% (area) fragmentation; grade 2, > 50% fragmentation; grade 3, 100% fragmentation, and diffuse mito::mCherry signal. Highly fragmented mitochondria refer to the sum of grade 2, grade 3, and the diffuse category. Data collected from two to four smaller cohorts of animals at indicated ages were pooled and presented as a single collection in the figures. Thus, for most of the percentile data in this work, the number of biological replica, for the practical purpose, is one. To avoid the possibility of spurious, singular observations, we assayed independent biological replica for mitochondrial morphology and touch sensitivity in the wild-type and the *mec-4* mutant. The results of analysis, available in Fig. S6, confirmed that data presented in this work were consistent and reproducible. To quantify roGFP signal intensity, projected z-stack confocal optical sections were taken, and mean roGFP pixel density was calculated by using ImageJ.

Molecular Biology and Plasmid Construction. Cloning and construction of plasmids were performed with standard molecular biology techniques. All expression constructs in the *twnEx* series transgenes were in the pPD95.77 Fire vector backbone, which contains the *unc-54* 3′-UTR for optimized expression in *C. elegans*. Primer sequence information is available upon request.

Protein Purification and in Vitro Kinase Assay. For purifying DRP-1 and UNC-43 proteins, 6xHis::GFP::DRP-1 or 6xHis::HA::UNC-43 were cloned into pIEx6 vector and were transfected by liposome into Sf9 cells. Cells were grown at 28 °C for 48 h and harvested by centrifugation at 100 × *g* for 10 min. After freezing by liquid nitrogen and stored at −80 °C overnight, cells were thawed and resuspended by 1/20 volume of lysis buffer (50 mM Tris·HCl, 300 mM NaCl, 10 mM imidazole) with 0.5% Triton X-100 (1% Triton X-100 for purifying UNC-43) and protease inhibitor mixture, without EDTA. This treatment was followed by homogenization with Dounce homogenizer and centrifugation 16,000 × *g* for 30 min at 4 °C, with additional sonication for UNC-43 purification. The supernatant was loaded onto Ni-NTA resin (Thermo), preequilibrated in the lysis buffer, and washed with 10× resin-bed volumes of wash buffer (50 mM Tris·HCl, 300 mM NaCl, 50 mM imidazole) to remove impurities. The protein was eluted with 500 μL of elution buffer (50 mM Tris·HCl, 300 mM NaCl, 500 mM imidazole).

To assay DRP-1 phosphorylation by UNC-43, 3 μg of purified GFP::DRP-1 (WT and T613A) and 1 μg of HA::UNC-43 (WT and E108K) proteins were incubated in 50 μL of kinase assay buffer containing 50 mM Hepes (pH 7.5), 8 mM $MgCl_2$, 2 mM $MnCl_2$, 0.1 mg/mL BSA, 1 μM recombinant calmodulin (Sigma), 0.5 mM $CaCl_2$, 50 μM ATP, and 10 μCi γ-[^{32}P] ATP at 25 °C for 10 min. Following kinase reaction, proteins were resolved by SDS/PAGE and substrate phosphorylation was detected by autoradiography.

Downloaded at Palestinian Territory, occupied on December 13, 2021
www.manaraa.com

ACKNOWLEDGMENTS. We thank Chun-Hao Chen, Keith Nehrke, Chiu-Ying Peng, and Ding Xue for reagents or strains; Jing-Chih Liu for assistance with in vitro kinase assay; Hsiu-Hsiang Lee and June-Tai Wu for access to the confocal microscope; Ya-Wen Liu for advice on protein purification; Sung-Tsang Hsieh and Ya-Wen Liu for suggestions on the manuscript; and Zuhang Sheng and Monica Driscoll for critically reading the manuscript and exchange of unpublished data. Some strains were provided by the *C. elegans* Genetics Center, which is funded by NIH Office of Research Infrastructure Programs Grant P40 OD010440, and by the National BioResources Project, Japan. This work is funded by National Health Research Institutes Grant NHRI-EX101-10119NC (to C.-L.P.), National Taiwan University Hospital Grant UN103-016 (to C.-C.C. and C.-L.P.), and Frontier Grant, Ministry of Science and Technology, Taiwan MOST 103-2321-B-001-058 (to R.-H.C.).

1. Wallace DC (2005) A mitochondrial paradigm of metabolic and degenerative diseases, aging, and cancer: A dawn for evolutionary medicine. *Annu Rev Genet* 39:359–407.
2. Chan DC (2012) Fusion and fission: Interlinked processes critical for mitochondrial health. *Annu Rev Genet* 46:265–287.
3. Scheckhuber CQ, et al. (2007) Reducing mitochondrial fission results in increased life span and fitness of two fungal ageing models. *Nat Cell Biol* 9(1):99–105.
4. Hughes AL, Gottschling DE (2012) An early age increase in vacuolar pH limits mitochondrial function and lifespan in yeast. *Nature* 492(7428):261–265.
5. Wilson PD, Franks LM (1975) The effect of age on mitochondrial ultrastructure. *Gerontologia* 21(2):81–94.
6. Yasuda K, et al. (2006) Age-related changes of mitochondrial structure and function in Caenorhabditis elegans. *Mech Ageing Dev* 127(10):763–770.
7. Chami M, et al. (2008) Role of SERCA1 truncated isoform in the proapoptotic calcium transfer from ER to mitochondria during ER stress. *Mol Cell* 32(5):641–651.
8. Spitzer NC (2012) Activity-dependent neurotransmitter respecification. *Nat Rev Neurosci* 13(2):94–106.
9. Burke SN, Barnes CA (2006) Neural plasticity in the ageing brain. *Nat Rev Neurosci* 7(1):30–40.
10. Burke SN, Barnes CA (2010) Senescent synapses and hippocampal circuit dynamics. *Trends Neurosci* 33(3):153–161.
11. Pan CL, Peng CY, Chen CH, McIntire S (2011) Genetic analysis of age-dependent defects of the Caenorhabditis elegans touch receptor neurons. *Proc Natl Acad Sci USA* 108(22):9274–9279.
12. Merrill RA, et al. (2011) Mechanism of neuroprotective mitochondrial remodeling by PKA/AKAP1. *PLoS Biol* 9(4):e1000612.
13. Han XJ, et al. (2008) CaM kinase I alpha-induced phosphorylation of Drp1 regulates mitochondrial morphology. *J Cell Biol* 182(3):573–585.
14. Toth ML, et al. (2012) Neurite sprouting and synapse deterioration in the aging Caenorhabditis elegans nervous system. *J Neurosci* 32(26):8778–8790.
15. Hanson GT, et al. (2004) Investigating mitochondrial redox potential with redox-sensitive green fluorescent protein indicators. *J Biol Chem* 279(13):13044–13053.
16. Youle RJ, Strasser A (2008) The BCL-2 protein family: Opposing activities that mediate cell death. *Nat Rev Mol Cell Biol* 9(1):47–59.
17. Chen CH, Chen YC, Jiang HC, Chen CK, Pan CL (2013) Neuronal aging: Learning from C. elegans. *J Mol Signal* 8(1):14.
18. Garigan D, et al. (2002) Genetic analysis of tissue aging in Caenorhabditis elegans: A role for heat-shock factor and bacterial proliferation. *Genetics* 161(3):1101–1112.
19. Hsu AL, Murphy CT, Kenyon C (2003) Regulation of aging and age-related disease by DAF-16 and heat-shock factor. *Science* 300(5622):1142–1145.
20. Kenyon C, Chang J, Gensch E, Rudner A, Tabtiang R (1993) A C. elegans mutant that lives twice as long as wild type. *Nature* 366(6454):461–464.
21. Kimura KD, Tissenbaum HA, Liu Y, Ruvkun G (1997) daf-2, an insulin receptor-like gene that regulates longevity and diapause in Caenorhabditis elegans. *Science* 277(5328): 942–946.
22. Tank EM, Rodgers KE, Kenyon C (2011) Spontaneous age-related neurite branching in Caenorhabditis elegans. *J Neurosci* 31(25):9279–9288.
23. O'Hagan R, Chalfie M, Goodman MB (2005) The MEC-4 DEG/ENaC channel of Caenorhabditis elegans touch receptor neurons transduces mechanical signals. *Nat Neurosci* 8(1):43–50.
24. Suzuki H, et al. (2003) In vivo imaging of C. elegans mechanosensory neurons demonstrates a specific role for the MEC-4 channel in the process of gentle touch sensation. *Neuron* 39(6):1005–1017.
25. Lee RY, Lobel L, Hengartner M, Horvitz HR, Avery L (1997) Mutations in the alpha1 subunit of an L-type voltage-activated Ca2+ channel cause myotonia in Caenorhabditis elegans. *EMBO J* 16(20):6066–6076.
26. Reiner DJ, Newton EM, Tian H, Thomas JH (1999) Diverse behavioural defects caused by mutations in Caenorhabditis elegans unc-43 CaM kinase II. *Nature* 402(6758): 199–203.
27. Satterlee JS, Ryu WS, Sengupta P (2004) The CMK-1 CaMKI and the TAX-4 Cyclic nucleotide-gated channel regulate thermosensory neuron gene expression and function in C. elegans. *Curr Biol* 14(1):62–68.
28. Labrousse AM, Zappaterra MD, Rube DA, van der Bliek AM (1999) C. elegans dynamin-related protein DRP-1 controls severing of the mitochondrial outer membrane. *Mol Cell* 4(5):815–826.
29. Kanazawa T, et al. (2008) The C. elegans Opa1 homologue EAT-3 is essential for resistance to free radicals. *PLoS Genet* 4(2):e1000022.
30. Ichishita R, et al. (2008) An RNAi screen for mitochondrial proteins required to maintain the morphology of the organelle in Caenorhabditis elegans. *J Biochem* 143(4):449–454.
31. Motori E, et al. (2013) Inflammation-induced alteration of astrocyte mitochondrial dynamics requires autophagy for mitochondrial network maintenance. *Cell Metab* 18(6):844–859.
32. Xie Q, et al. (2015) Mitochondrial control by DRP1 in brain tumor initiating cells. *Nat Neurosci* 18(4):501–510.
33. Kurashima K, Chae M, Inoue H, Hatakeyama S, Tanaka S (2013) A uvs-5 strain is deficient for a mitofusin gene homologue, fzo1, involved in maintenance of long life span in Neurospora crassa. *Eukaryot Cell* 12(2):233–243.
34. Brenner S (1974) The genetics of Caenorhabditis elegans. *Genetics* 77(1):71–94.
35. Mello CC, Kramer JM, Stinchcomb D, Ambros V (1991) Efficient gene transfer in C. elegans: Extrachromosomal maintenance and integration of transforming sequences. *EMBO J* 10(12):3959–3970.

Downloaded at Palestinian Territory, occupied on December 13, 2021

www.manaraa.com